



Conjugates of desferrioxamine and aromatic amines improve markers of iron-dependent neurotoxicity

Rodrigo R. V. Carvalho · Tanara V. Peres · Cleber W. Liria · M. Teresa Machini · Michael Aschner · Breno P. Espósito

Received: 27 May 2020 / Accepted: 27 November 2020 / Published online: 3 January 2021
© The Author(s), under exclusive licence to Springer Nature B.V. part of Springer Nature 2021

Abstract Alzheimer's Disease (AD) is a complex neurodegenerative disorder associated in some instances with dyshomeostasis of redox-active metal ions, such as copper and iron. In this work, we investigated whether the conjugation of various aromatic amines would improve the pharmacological efficacy of the iron chelator desferrioxamine (DFO). Conjugates of DFO with aniline (DFOANI), benzosulfanylamide (DFOBAN), 2-naphthalenamine (DFONAF) and 6-quinolinamine (DFOQUN) were obtained and their properties examined. DFOQUN

had good chelating activity, promoted a significant increase in the inhibition of β -amyloid peptide aggregation when compared to DFO, and also inhibited acetylcholinesterase (AChE) activity both in vitro and in vivo (*Caenorhabditis elegans*). These data indicate that the covalent conjugation of a strong iron chelator to an AChE inhibitor offers a powerful approach for the amelioration of iron-induced neurotoxicity symptoms.

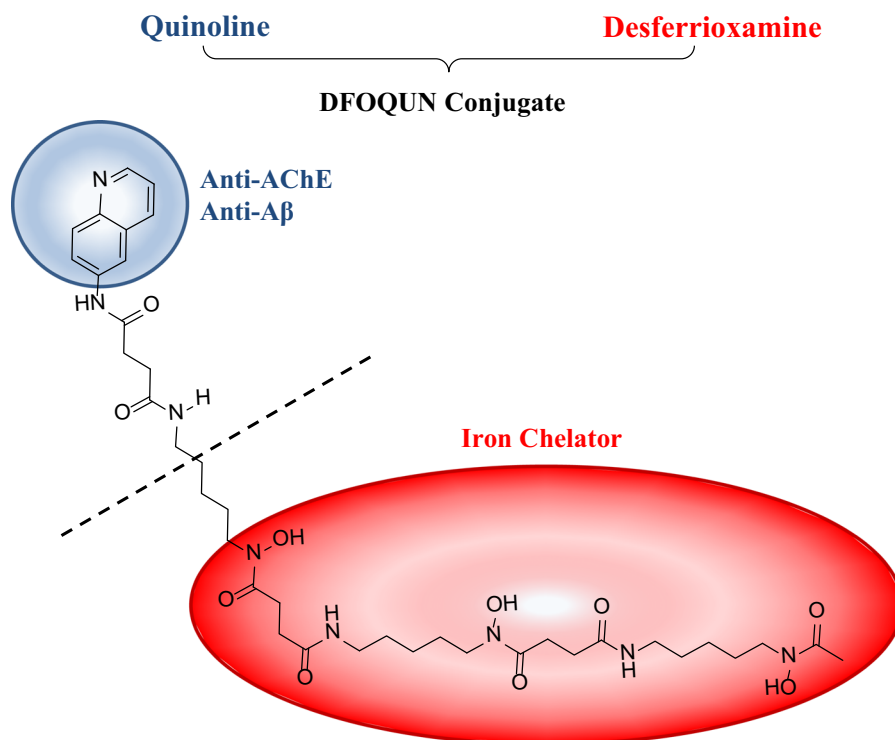
Supplementary information The online version of this article (<https://doi.org/10.1007/s10534-020-00277-7>) contains supplementary material, which is available to authorized users.

R. R. V. Carvalho (✉) · B. P. Espósito
Department of Fundamental Chemistry, Institute of Chemistry, University of São Paulo, São Paulo, SP, Brazil
e-mail: rodrigovictor65@hotmail.com

T. V. Peres · M. Aschner
Department of Molecular Pharmacology, Albert Einstein College of Medicine, Bronx, NY, USA

C. W. Liria · M. T. Machini
Department of Biochemistry, Institute of Chemistry, University of São Paulo, São Paulo, SP, Brazil

Graphic abstract



Keywords Desferrioxamine · Iron · Alzheimer's disease · Acetylcholinesterase · Beta amyloid · *Caenorhabditis elegans*

Introduction

Iron (Fe), the fourth most abundant element in the earth's crust, has many roles in biological systems, mostly derived from its capacity to mediate the traffic of electrons in redox reactions and to form reversible complexes with molecular oxygen that are crucial to biochemical processes, such as ATP or DNA synthesis and oxygen transport (Ward et al. 2015). However, precisely due to its ability to catalyze electron transfer reactions in an oxygenated environment, whenever in excess and/or outside its assigned biochemical compartments, iron will behave as a potent toxin (Breuer et al. 2000; Cabantchik et al. 2013; Knutson 2019). Indeed, excess of this metal in the bloodstream leads, for example, to labile plasma iron (LPI) formation, which enhances the levels of intracellular pools of

reactive iron and generation of reactive oxygen species (ROS) that will damage organs, such as pancreas, heart, liver and brain (Cabantchik et al. 2013). Iron overload is a common complication of diseases such as hereditary hemochromatosis and thalassemias. The risks of complications associated with excess iron in neurodegenerative disorders may be increased due the oxidation of lipids, proteins and enzymes, as well as destruction of RNA and DNA (Hider et al. 2011). Hence, oxidative stress may disturb iron homeostasis and damage neuronal cells (Rodríguez-Rodríguez et al. 2012). The brain is particularly vulnerable to damage caused by oxidative stress due to its high oxygen consumption, low concentration of antioxidants and its propensity to accumulate metals over time (Rodríguez-Rodríguez et al. 2012).

These factors may be relevant to the development of Alzheimer's Disease (AD). AD is a complex neurodegenerative disorder associated with memory loss and decline of cognitive functions, promoting dementia in the elderly. It is a fatal, incurable disorder, which affects over 36 million people in the world

(Rodríguez-Rodríguez et al. 2012). Due to population aging, it is estimated that this figure will increase to 66 million by 2030 and 115 million by 2050 (Rodríguez-Rodríguez et al. 2012). In the search for a cure, different targets have been identified and studied. Inhibition of the production and deposition of β -amyloid ($A\beta$) peptide, which causes the accumulation of neurotoxic senile plaques in the brain (Hayne et al. 2014), and inhibition of acetylcholinesterase (AChE) (Berg et al. 2011; Tiiman et al. 2013), the enzyme responsible for the rapid conversion of acetylcholine to choline and acetic acid required in the termination of impulse transmission, have been the main approaches to anti-AD therapy. Only five drugs have been approved by the US Food and Drug administration (FDA) for the treatment of AD symptoms: tacrine, donepezil, rivastigmine, galantamine (cholinesterase inhibitors) and memantine (NMDA receptor antagonist) (Colović et al. 2013; Schneider 2000).

There is ample evidence linking increased iron brain levels and $A\beta$ aggregation. Both Fe(II) and Fe(III) can form hexacoordinated complexes with $A\beta$ through Asp, Glu and His residues (Kozłowski et al. 2012). Conversely, chelation therapy disrupts metal- $A\beta$ interaction (Keri et al. 2013, 2016; Quintanova et al. 2015b). One of the most specific iron chelators is desferrioxamine (DFO), a siderophore secreted by the microorganism *Streptomyces pilosus* and employed in the treatment of iron overload disorders (Kurth et al. 2016). DFO forms a kinetically inert, strong hexadentate complex with excess iron, which is readily excreted (Kurth et al. 2016). However, DFO is highly hydrophilic, with poor cell permeability that makes its traffic through the blood–brain barrier (BBB) unlikely (Heli et al. 2011; Pramanik et al. 2019; Raines et al. 2015; Sheth 2014).

The multifactorial nature and complexity of AD has challenged scientists searching for new anti-AD drugs. To this end, the strategy of multi-target-directed-ligands (MTDL) has been explored to develop new anti-AD candidates. MTDL is based on conjugation of one or more molecules with other pharmacophoric moieties in order to enhance their pharmacological properties (Santos et al. 2016). Our research group used this strategy to create new DFO conjugates such as DFCAF and DFO-TAT peptide, which are DFO derivatives with enhanced lipophilicity and cell permeability (Alta et al. 2014; Goswami et al. 2014).

In this study, we coupled the aromatic amines aniline, 2-naphthalenamine, 6-quinolinamine (analogue of the AChE inhibitor tacrine) and benzosulfanilamide to obtain four new DFO conjugates (Fig. 1) and evaluated their effects on biochemical markers relevant to AD therapy. These molecules were selected due their ability to introduce π – π stacking interactions with AD targets similar to other drugs (Chen et al. 2018a, b; Martinez and Iverson 2012; Piemontese et al. 2018; Riwar et al. 2017; Thakuria et al. 2019). As molecule designers, our rationale is always to prepare a single molecule with dual activity, rather than relying on the administration of two different treatments. This approach decreases the risks and complications inherent to polytherapies (Palleria et al. 2013), while developing synthetic strategies to impart new functions to established chelators. In addition, a succinic spacing group was introduced between the chelator and the aromatic amine moieties in our conjugates, thus making it impossible to adequately compare the effects of the final product and their constituting parts alone.

Experimental section

Chemicals

All chemicals were at least 99% pure and used without further purification. Desferrioxamine mesylate (DFO) was obtained from Cristália (Brazil). Ferrous ammonium sulfate (FAS), aniline, calcein, benzosulfanylamide, 6-quinolinamine, 2-naphthalenamine and other chemicals were purchased from Sigma Aldrich (USA), unless otherwise noted. Trifluoroacetic acid, analytical TLC plates pre-coated with silica gel and chromatographic grade solvents used for RP-HPLC and LC–MS were from Merck (USA). Dihydrorhodamine chloride was obtained from Biotium (USA).

Instruments

Elemental analysis was performed in a CHN 2400 (Perkin Elmer, Waltham, USA). Melting points were determined in a Kofler Apparatus (Fisher Scientific, Loughborough, United Kingdom). NMR spectra were recorded in a Varian Inova (Oklahoma, USA) or Bruker DRX Spectrometer (Bruker, Billerica, USA) operating at 300 MHz and 500 MHz, respectively (for

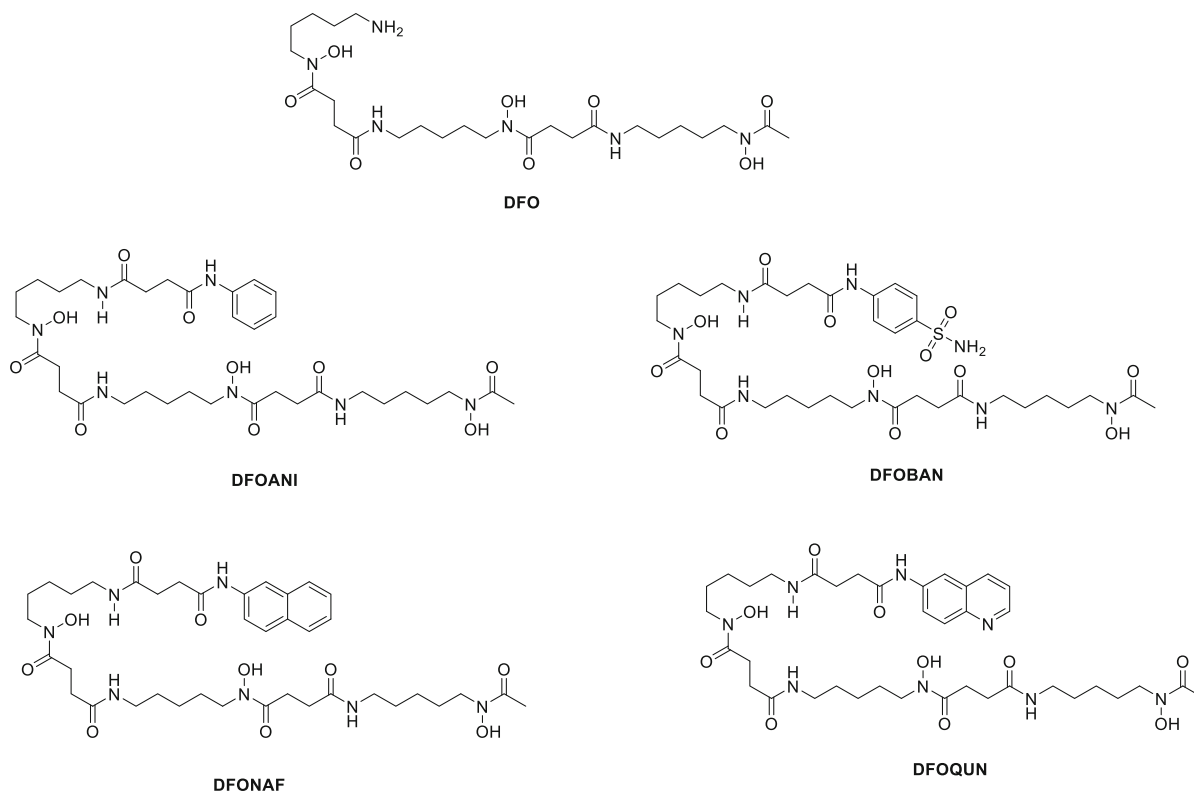


Fig. 1 Structures of DFO and the DFO conjugates prepared in this study

^1H NMR), or 75 MHz and 128 MHz, respectively (for ^{13}C NMR). NMR spectra were calibrated using DMSO- d_6 solvent signals ($\delta_{\text{H}} = 2.50$ and $\delta_{\text{C}} = 39.52$) and reported in ppm. Mass spectra of carboxylic acids were recorded in an Amazon Speed ETD—Bruker (Germany). The capillary voltage of the electrospray ionization source (ESI) was set to 4.5 kV. The capillary temperature was set at 200 °C. Nebulizer pressure was set to 12 psi. Fluorescence and electronic absorbance measurements were conducted in the microplate readers SpectraMax M4 (Molecular Devices, Sunnyvale, USA) or FluoStar Optima (BMG, Ortenberg, Germany). Chromatographic purification by preparative reverse-phase HPLC was carried in a RP-HPLC system from Waters (Millford, MA, USA) composed of pump (Waters Delta 600 pump), pump controller (Waters 600 Controller), one UV detector (Waters 2487 Dual λ Absorbance detector), a manual injector sample (Rheodyne 7725), a recorder (Kipp & Zonen Servogor 124 recorder) and a Vydac C_{18} column (10 μm , 300 Å, 2.2 \times 25 cm). The characterization by LC–MS was carried out with a

Shimadzu Corporation RP-HPLC system (Kyoto, Japan, flow 0.8 mL/min) composed of a DGU model degasser 20A₃, two pumps model LC-20AD, one Rheodyne 8125 injector, one column oven model CTO-20A ($T = 32$ °C), one C_{18} column (0.46 cm \times 25.00 cm, 5 μm particle diameter, 300 Å pore diameter; Grace-Vydac, Hesperia, CA, USA) and a UV/Vis detector model SPD-20A. This RP-HPLC system is coupled to a Bruker Daltonics (Fahrenheitstrasse, Germany) AmaZon X mass spectrometer with electrospray ionization source, positive ESI mode and an ion trap analyzer. The capillary voltage was 4500 V and the end-plate offset voltage was 500 V (for positive mode) and 220 °C. For spectrum analysis the HyStar 3.2 software was used.

Synthesis of carboxylic acids

2a, *2b* and *4*: The syntheses were based on previously described methods (Balakrishna et al. 2014). Distilled water (5 mL) was mixed with the appropriate amine (aniline or benzosulfanylmide to obtain *2a* or *2b*;

1 mmol) and stirred constantly. Three portions of succinic anhydride (1 mmol, 1 mmol and 0.6 mmol) were added to the mixture with 1 min intervals between them. The reaction mixture was stirred for 10 min at room temperature and under open air. The white precipitate was washed with deionized water and dried under vacuum for 24 h to achieve the desired product. To obtain 4, distilled water (50 mL) was mixed with 2-naphthylamine (10 mmol) and succinic anhydride (10 mmol). The reaction mixture was stirred for 15 min at room temperature and under open air. The brown precipitate was washed with concentrated acetic acid, distilled water and dried under vacuum for 24 h to achieve the desired product. The reactions were monitored by TLC using chloroform/ acetic acid/methanol (85:10:5) eluent.

6: The synthesis was based on a previous report (Sinha and Shrivastava 2013). 6-quinolinamine (2 mmol) and succinic anhydride (2 mmol) were mixed in 15 mL toluene and stirred constantly in reflux under nitrogen. After 4 h, the yellow solid was washed with $\text{CHCl}_3/\text{MeOH}$ (95:5) and dried under vacuum for 24 h to achieve the desired product. The reaction was monitored by TLC using chloroform/ acetic acid/methanol (85:10:5) eluent.

4-oxo-4-(phenylamino)butanoic acid (2a): Yield: 70%. **m.p.:** 144–146 °C. **R_f:** 0.43. **¹H-NMR** (300 MHz, DMSO-d_6): δ (ppm) 12.10 (s, 1H), 9.92 (s, 1H), 7.61–7.51 (m, 2H), 7.33–7.20 (m, 2H), 7.06–6.94 (m, 1H), 2.61–2.47 (m, 4H). **¹³C RMN** (75 MHz, DMSO-d_6): δ (ppm) 174.25, 170.48, 139.72, 129.09, 123.33, 119.32, 31.47, 29.24. **ESIMS (m/z):** 192 (M–H)[–].

4-oxo-4-((4-sulfamoylphenyl)amino)butanoic acid (2b): Yield: 0.50% **m.p.:** 204–205 °C **R_f:** 0.10. **¹H-NMR** (300 MHz, DMSO-d_6): δ (ppm) 12.14 (s, 1H), 10.29 (s, 1H), 7.72 (s, 4H), 7.22 (s, 2H), 2.65–2.47 (m, 4H). **¹³C RMN** (75 MHz, DMSO-d_6): δ (ppm) 174.19, 171.17, 142.58, 138.47, 127.12, 118.84, 31.55, 29.07 **ESIMS (m/z):** 273 (M + H)⁺

4-(naphthalen-2-ylamino)-4-oxobutanoic acid (4): Yield: 35% **m.p.:** 194–195 °C **R_f:** 0.50 **¹H-NMR** (300 MHz, DMSO-d_6): δ (ppm) 12.17 (s, 1H), 10.18 (s, 1H), 8.30 (d, $J = 2.1$ Hz, 1H), 7.88–7.73 (m, 3H), 7.56 (dd, $J_1 = 8.9$, $J_2 = 2.1$ Hz, 1H); 7.41 (dddd, $J_1 = 6.9$, $J_2 = 8.0$, $J_3 = 6.8$, $J_4 = 1.3$ Hz, 2H), 2.69–2.50 (m, 4H) **¹³C RMN** (75 MHz, DMSO-d_6): δ (ppm) 174.34, 170.86, 137.28, 133.90, 130.03,

128.75, 127.87, 127.66, 126.82, 124.88, 120.25, 115.27, 31.12, 29.23. **ESIMS (m/z):** 244 (M + H)⁺

4-oxo-4-(quinolin-6-ylamino)butanoic acid (6): Yield: 82% **m.p.:** 230–232 °C **R_f:** 0.30 **¹H-NMR** (300 MHz, DMSO-d_6): δ (ppm) 12.14 (s, 1H), 10.33 (s, 1H), 8.75 (dd, $J_1 = 4.2$, $J_2 = 1.7$ Hz, 1H); 8.38 (d, $J = 2.3$ Hz, 1H), 8.24 (dd, $J = 8.3$, 1.7 Hz, 1H), 7.94 (d, $J = 9.1$ Hz, 1H); 7.76 (dd, $J_1 = 9.1$, $J_2 = 2.4$ Hz, 1H), 7.45 (dd, $J = 8.3$, 4.2 Hz, 1H), 2.69–2.50 (m, 4H). **¹³C RMN** (75 MHz, DMSO-d_6): δ (ppm) 174.32, 171.09, 149.29, 144.96, 137.58, 135.89, 129.87, 128.80, 123.62, 122.19, 115.04, 31.55, 29.20. **ESIMS (m/z):** 245 (M + H)⁺

General procedure for the synthesis of DFO conjugates

DFO conjugates were prepared based on previous reports (Liu et al. 2010). In DMF (15 mL), 1 mmol of the carboxylic acids were mixed with DFO (1 mmol), EDC (1.5 mmol) and HOBT (1.5 mmol). The mixture was stirred constantly and heated to 50 °C for 5 min. After the reagents dissolved, DIPEA (2 mmol) was added to the solution and the mixture was stirred for 16 h at room temperature under nitrogen. The solid was washed with diethyl ether, distilled water and methanol. The reactions were monitored by TLC using chloroform/methanol (80:20) eluent.

Purification and characterization of DFO conjugates

Purification by preparative reverse-phase HPLC was carried in a RP-HPLC with two eluents: A (trifluoroacetic acid 0.1% in water) and B (60% acetonitrile, 0.09% trifluoroacetic acid in water). A sample of 250 mg of crude conjugate was injected and the elution sequence was 20% B for 15 min, 20–60% B in 60 min, 60–95% B in 15 min, 95% B for 5 min. The fractions were analyzed by direct infusion mass spectrometry and those containing the desired conjugate were pooled and lyophilized. Analysis of the purified conjugate, at the concentration 1 mg/mL in DMSO, was carried out in a LC–MS system using the same eluents described above. The gradient applied was 5 to 95% B in 30 min, the capillary voltage was 4500 V and the end plate offset voltage was 500 V (for positive mode).

DFOANI: Yield: 26.7% m.p: 180–182 °C. **R_f**: 0.52. **¹H-NMR** (500 MHz; DMSO) δ(ppm) 9.92 (s; 1H), 9.66 (s; 1H), 9.61 (s; 2H), 7.84 (t; J = 5.4 Hz; 1H); 7.78 (t; J = 5.3 Hz; 2H), 7.57 (d; J = 7.7 Hz; 2H); 7.27 (t; J = 7.9 Hz; 2H), 7.01 (t; J = 7.4 Hz; 1H), 3.45 (t; J = 6.4 Hz; 6H), 3.05–2.96 (m; 6H), 2.58 (t; J = 7.1 Hz; 3H), 2.54 (dd; J = 9.4; 5.1 Hz; 3H), 2.39 (t; J = 7.3 Hz; 2H), 2.27 (t; J = 7.2 Hz; 4H), 1.97 (d; J = 5.0 Hz; 3H), 1.51 (dd; J = 22.7; 16.1 Hz; 6H); 1.37 (d; J = 6.8 Hz; 6H), 1.22 (d; J = 6.7 Hz; 6H). **¹³C RMN** (126 MHz., DMSO) δ (ppm) 172.44, 171.78, 171.49, 170.96, 139.80, 129.11, 123.33, 119.37, 47.55, 47.25, 38.90, 32.23, 30.80, 30.37, 29.28, 28.03, 26.49, 23.96, 20.82. **ESIMS (m/z):** 736 (M + H)⁺. **Elemental Formula** C₃₅H₅₇N₇O₁₀. **Calculated (%)**: C 57.1, H 7.8, N 13.3, **Found (%)**: C 55.6, H 7.9, N 12.9, **Experimental Formula:** C₃₅H₅₇N₇O₁₀.0.4CH₃.OH.0.95H₂O. ε **[DFOANI(Fe)] complex** (λ_{max} = 430 nm): 2037.3 L mol⁻¹ cm⁻¹.

DFOBAN: Yield: 24.9% m.p: 184–185 °C. **R_f**: 0.0.25 **¹H-NMR** (500 MHz; DMSO) δ(ppm) 10.28 (s, 1H), 9.66 (s, 1H), 9.61 (s, 2H), 7.85 (t, J = 5.5 Hz, 1H), 7.77 (t, J = 5.3 Hz, 2H), 7.74 (d, J = 9.5 Hz, 4H), 7.23 (s, 2H), 3.45 (t, J = 7.0 Hz, 6H), 3.06–2.95 (m, 6H), 2.63–2.53 (m, 6H), 2.43–2.36 (m, 2H), 2.27 (t, J = 7.1 Hz, 4H), 1.96 (s, 3H), 1.55–1.44 (m, 6H), 1.42–1.34 (m, 6H), 1.22 (d, J = 6.8 Hz, 6H). **¹³C RMN** (126 MHz., DMSO) δ (ppm) 172.44, 171.61, 171.37, 142.68, 138.44, 127.13, 118.84, 47.55, 47.25, 32.21, 30.51, 30.37, 29.28, 28.03, 26.50, 23.96, 20.82. **ESIMS (m/z):** 815 (M + H)⁺. **Elemental Formula** C₃₅H₅₈N₈O₁₂S. **Calculated (%)**: C 51.8, H 7.2, N 13.8 **Found (%)**: C 50.8, H 7.2, N 13.2 **Experimental Formula:** C₃₅H₅₈N₈O₁₂S.0.55CH₃OH.0.45H₂O ε **[DFOBAN(Fe)] complex** (λ_{max} = 430 nm): 1642.7 L mol⁻¹ cm⁻¹.

DFONAF: Yield: 43.8% m.p: 180–182 °C. **R_f**: 0.6 **¹H-NMR** (500 MHz; DMSO) δ(ppm) 10.14 (s, 1H), 9.65 (s, 1H), 9.61 (s, 2H), 8.29 (s, 1H), 7.89–7.75 (m, 6H), 7.59–7.54 (m, 1H), 7.49–7.42 (m, 1H), 7.41–7.35 (m, 1H), 3.45 (t, J = 7.0 Hz, 6H), 3.01 (td, J = 13.2, 6.6 Hz, 6H), 2.64–2.52 (m, 6H), 2.43 (t, J = 7.2 Hz, 2H), 2.27 (t, J = 6.6 Hz, 4H), 1.97 (s, 3H), 1.49 (d, J = 6.3 Hz, 6H), 1.39 (dq, J = 14.8, 7.5 Hz, 6H), 1.22 (d, J = 6.2 Hz, 6H). **¹³C RMN** (126 MHz., DMSO) δ (ppm) 172.44, 171.78, 171.49, 171.28, 137.38, 133.93, 130.05, 128.74, 127.89, 127.68, 126.82, 124.87, 120.33, 115.28, 47.55, 47.25, 38.92, 38.89, 32.29, 30.79, 30.37, 29.28, 28.03, 26.50, 23.96, 20.82.

ESIMS (m/z): 786 (M + H)⁺. **Elemental Formula** C₃₉H₅₉N₇O₁₀ **Calculated (%)**: C 59.6 H 7.6 N 12.5 **Found (%)**: C 59.9 H 7.9 N 12.0 **Experimental Formula:** C₃₉H₅₉N₇O₁₀.0.1CH₃OH.

DFOQUN: Yield: 24.3% m.p: 143–145 °C. **R_f**: 0.5 **¹H-NMR** (500 MHz; DMSO) δ(ppm) 10.38 (s, 1H), 9.63 (s, 2H), 8.85 (dd, J = 4.4, 1.5 Hz, 1H), 8.52–8.37 (m, 2H), 8.01 (d, J = 9.1 Hz, 1H), 7.85 (dd, J = 9.1, 2.3 Hz, 2H), 7.77 (t, J = 5.4 Hz, 2H), 7.60 (dd, J = 8.4, 4.5 Hz, 1H), 3.01 (dq, J = 13.2, 6.7 Hz, 8H), 2.67–2.53 (m, 8H), 2.42 (q, J = 6.9 Hz, 4H), 2.26 (t, J = 7.1 Hz, 5H), 1.95 (s, 3H), 1.54–1.44 (m, 6H), 1.41–1.33 (m, 6H), 1.26–1.12 (m, 6H). **¹³C RMN** (126 MHz., DMSO) δ (ppm) 172.43, 171.79, 171.67, 171.42, 147.89, 138.31, 129.11, 128.42, 128.00, 124.84, 122.32, 114.99, 47.53, 47.24, 38.89, 32.25, 30.64, 30.39, 29.28, 28.02, 26.48, 23.94, 20.79. **ESIMS (m/z):** 787 (M + H)⁺. **Elemental Formula** C₃₈H₅₈N₈O₁₀ **Calculated (%)**: C 58.0 H 7.4 N 14.2 **Found (%)**: C 58.3 H 7.5 N 14.1 **Experimental Formula:** C₃₈H₅₈N₈O₁₀ ε **[DFOQUN(Fe)] complex** (λ_{max} = 430 nm): 1231.8 L mol⁻¹ cm⁻¹.

Calcein competition studies

The ability of the new chelators to scavenge iron was studied by competition against the fluorescent chelator calcein, according to published protocols (Espósito et al. 2002a). Aliquots of 190 μL of ferric calcein (CAFe; 2 μM) in HBS/Chelex (Hepes Buffered Saline; hepes 20 mM, NaCl 150 mM, Chelex 1 g/100 mL; pH 7.4) were added to transparent 96-well microplates. Next, 10 μL of conjugates (final concentrations: 0–15 μM) in DMSO were added to each well. Fluorescence was recorded after 2 h incubation at 37 °C in a BMG FluoStar Optima microplate reader (λ_{exc}/λ_{em} = 485/520 nm). Two independent assays were performed, each one in duplicate.

DHR antioxidant activity

The ability of the new chelators to block iron-dependent oxidation of DHR was studied according to previous methods (Espósito et al. 2003). Aliquots of 10 μL of ferric nitrilotriacetate (Fe(NTA)) were added to transparent 96 wells microplates followed by 10 μL of the conjugates (0–300 μM) in DMSO. Next, 180 μL of fluorogenic mixture (DHR 50 μM and ascorbic acid 40 μM in HBS/Chelex) were transferred to the wells.

Final concentrations of Fe(NTA) and conjugates were 2 μM and 0–15 μM , respectively, with 5% final DMSO. The fluorescence was measured in a BMG Fluostar Optima ($\lambda_{\text{exc}}/\lambda_{\text{em}} = 485/520 \text{ nm}$) at 37 °C for 1 h. Two independent assays were performed, each one in duplicate.

DPPH anti-oxidant activity

Aliquots of 10 μL of DFO conjugates (0–2 mM) dissolved in DMSO were added to 96-well microplates, followed by addition of 190 μL of DPPH (0.1 mM in methanol) (Molyneux 2004). Final concentrations of conjugates were 0–100 μM and final DMSO percentage was 5%. The microplates were incubated for 30 min at room temperature in the dark and the absorbance ($\lambda = 520 \text{ nm}$) was measured in a SpectraMax M4 microplate reader. Antioxidant activity was calculated according to the equation:

$$AA(\%) = \frac{(\text{Abs DPPH} - \text{Abs Sample})}{(\text{Abs DPPH})} \times 100$$

where AA(%) is the percentage of antioxidant activity. Two independent assays were performed, each one in duplicate.

Fe(II) speciation calculation

CHEAQS NEXT® is a computational software used for chemical equilibrium calculations in aqueous systems, widely used in geological and environmental studies (Walaszek et al. 2018). The interest in calculating Fe(II) speciation was to estimate the levels of bioavailable iron that can affect worm mortality. Speciation calculation was performed considering ionic strength of 0.09 M, pE of 0.9128 (54 mV), FeSO_4 6.2 mM (at $\frac{1}{2}$ LC50) and H^+ 1.1 μM (free activity), allowing for the formation of insoluble species (Xie et al. 2009).

Inhibition of $\text{A}\beta_{1-42}$ aggregation

To investigate the inhibition of $\text{A}\beta_{1-42}$ aggregation by the DFO conjugates in the presence and absence of Fe, an assay was performed using the fluorescent probe Thioflavin-T (ThT). When ThT binds to the peptide structure, the probe fluoresces. Any anti-Alzheimer drug candidate would be expected to disrupt the

aggregation of the peptide, which in this test would be equivalent to releasing the probe into the aqueous medium and quenching its fluorescence. According to the methodology (Guzior et al. 2015), the $\text{A}\beta_{1-42}$ fragment (Sigma Aldrich A9810) was solubilized in DMSO to obtain a 100 μM stock solution and then diluted in PBS pH 7.4 to 5 μM (containing 5% DMSO). Tacrine, DFO and DFOQUN were dissolved in DMSO (15 mM) and diluted in PBS (100 μM). Finally, aliquots of 20 μL $\text{A}\beta_{1-42}$ (5 μM), 20 μL conjugate (100 μM) and 4 μL FeSO_4 (50 μM) were transferred to a 96-well black microplate. Each well was filled with PBS, at a final volume of 100 μL . The microplate was incubated in the dark under constant shaking at room temperature for 24 h. After incubation, 2 μL of ThT solution (44.4 μM in PBS) was transferred to each well. The microplate was inserted into a Spectra Max M4 reader and the fluorescence was recorded ($\lambda_{\text{exc}}/\lambda_{\text{em}} = 446/490 \text{ nm}$). Final concentrations of $\text{A}\beta_{1-42}$, compounds, FeSO_4 and ThT were 1, 20, 2 and 1 μM , respectively, and final DMSO percentage equal to 1%. The aggregation inhibition percentage was calculated according to the following equation (Hiremathad et al. 2016):

$$I(\%) = (1 - F_i/F_o) \times 100$$

where F_i Fluorescence of treated $\text{A}\beta_{1-42}$, F_o Fluorescence of $\text{A}\beta_{1-42}$, I(%) percentage of inhibition. Three independent assays were performed, each in triplicate.

C. elegans strain and maintenance

N2 nematodes were acquired from the Caenorhabditis Genetics Center (CGC—University Minnesota, Twin Cities, MN, USA). Worms were cultivated at 20 °C in standard culture conditions in plastic petri dishes containing agar 8P (Bianchi and Driscoll 2006). Synchronized populations at the L1 larval stage were obtained by isolation of eggs of gravid hermaphrodites using bleach solution as previously described (1% NaOCl, 0.25 M NaOH) (Kenyon 1988). Eggs were hatched in NGM plates without food. For all the experiments, synchronized worms were washed from the hatching plates, treated and then transferred to NGM plates containing nematode growth medium and *E. coli* OP50 strain as food (Brenner 1974).

Lethality assay

The worms were treated with various concentrations of FeSO₄ to determine the LC₅₀. After synchronization, 2500 worms in the L1 stage were treated with Fe (0–100 mM) for 1 h in NaCl (0.5%) solution at 20 °C. Then, 30–50 worms were washed and transferred to NGM plates with bacteria. After 48 h, the number of living worms was counted. Three independent assays were performed each in triplicate.

Survival assay

We found the LC₅₀ to be equal to 12.5 mM. In order to have the least possible number of worms dying while observing toxicity, we used an iron concentration of 6.2 mM (1/2 LC₅₀) in all subsequent assays. The same procedures for lethality assays were employed, but after the addition of iron, we co-administered DFO. We studied both the effects of DFO concentration and DMSO percentage. Three DFO concentrations were studied (1: 2.5 μM with 0.015% DMSO; 2: 5 μM with 0.03% DMSO; 3: 10 μM with 0.06% DMSO). Survival rate was improved under condition 2. Accordingly, survival and subsequent assays were carried out at the L1 stage with DFO and other chelators under the following conditions: Fe (6.2 mM), chelator (5 μM) and DMSO (0.03%). DMSO was not toxic to *C. elegans* up to a 10% level (Espósito et al. 2020).

AChE activity in *C. elegans* (in vivo assay)

After treating the worms with Fe and conjugates (in suspensions of 20,000 worms/500 μL in Eppendorf tubes), we quantified the activity of AChE in wild-type (N2) worms. Worms were washed with NaCl (0.5%) to remove bacteria. Samples were frozen 4 consecutive times in acetone/dry ice bath and sonicated three times on ice at 15 s intervals using 40% amplitude. Then, samples were centrifuged at 14,000 rpm for 30 min to remove insoluble residues. The supernatant was assayed for AChE levels with the Amplex Red ACh/AChE assay kit (Invitrogen A12217) according to the manufacturer's instructions. Absorbance was measured in a BMG Fluostar Optima reader ($\lambda_{exc}/\lambda_{em} = 544/590$ nm). Three independent experiments were performed in triplicate and final fluorescence was

normalized to protein content, quantified by the Bradford method (Hart 2006; Sashidhara et al. 2014b).

AChE activity (in vitro assay)

Ten μL of conjugate solutions (0–300 μM) dissolved in HBS (DMSO 6.7%) were transferred to 96-well black microplates. Next, 10 μL FeSO₄ (300 μM), 10 μL acetylcholine (300 μM) and 70 μL HBS buffer were added to each well, and received 100 μL of the reagent mixture (400 μM amplex red and 1 U/mL AChE, without acetylcholine) of the assay kit described above. The final concentration of the conjugates was 0–15 μM and the final DMSO percentage was 0.1%. The microplate was incubated at room temperature in the dark for 30 min and fluorescence was measured using BMG Fluostar Optima ($\lambda_{exc}/\lambda_{em} = 544/590$ nm). Three independent assays were performed, each in triplicate.

Body bend assay

The behavior of the nematode reflects the activity of its central nervous system, which depends on several factors such as external stimulus, neuronal structure and changes in the animal environment (Hart 2006). In addition to its effects on cognitive function, acetylcholine acts on neuromuscular junctions in the CNS. In *C. elegans*, acetylcholine functions to increase locomotion secondary to muscle contraction (Gjorgjieva et al 2014). Reactive oxygen species generated by iron damage the cholinergic system, interrupting the communication between motor neurons and muscle cells in the worm. The number of body bends was selected for analysis of locomotion. Worms were transferred to NGM plates and the number of body bends was counted with a stereomicroscope. Two types of treatment were used after exposure of the L1 worms to Fe and chelators. In treatment 1, worms were transferred to 60 mm Petri dishes without food and body curvature counted for a period of 20 s. In treatment 2, worms were transferred to 60 mm Petri dishes with food, and after a 2 h period, again transferred to plates without food for counting the curvatures for the same period. Analyses were carried out in at least ten worms per group, in triplicate. Assays were repeated independently three times.

log P calculation

Lipophilicity is the tendency of a compound to be dissolved preferentially in an apolar phase over an aqueous phase. This information is usually presented as partition coefficient (P). The log P value of the conjugates was calculated by the Marvin Sketch 16.6.27.0 software (<https://chemaxon.com/products/marvin>). The standard software method was used for the calculations, based on the contribution of all atoms to generate the log P. The concentrations of Na⁺, Cl⁻ and K⁺ cations were defined as 0.1 M (Arndt et al. 2017).

Statistical analysis

In the case of biological assays, statistical analyses were performed using the Graph Pad Prism 6.0 software (<https://www.graphpad.com/scientific-software/prism/>) with one-way ANOVA followed by Tukey's post hoc test. Results were expressed as Means ± Standard Deviation (SD) and differences were considered significant when $p < 0.05$. $n = 2$ or 3 was used as effects were statistically significant even with few replicates, as occurs with other drug tested in *C. elegans* (e.g., Sashidhara et al. 2014a, b; Chand et al. 2018; Maqbool et al. 2020).

Results and discussion

Synthesis, purification and lipophilicity of the conjugates

Succinylation of the aromatic amines in water and open air was adapted from a previously described method (Balakrishna et al. 2014) to obtain the carboxylic acid derivatives of aniline (2a; yield: 70%), benzosulfanylamine (2b; yield: 50%) and 2-naphthalenamine (4; yield: 35%). Increasing reaction time and/or succinic anhydride concentration did not increase the yield of 4 (data not shown), probably due to resonance effects over the extended ring system that decreased the reactivity of the aromatic amine. The method above did not work for the preparation of the carboxylic derivative of 6-quinolinamine (6); this product was obtained in high yield (82%) only when toluene was used under reflux.

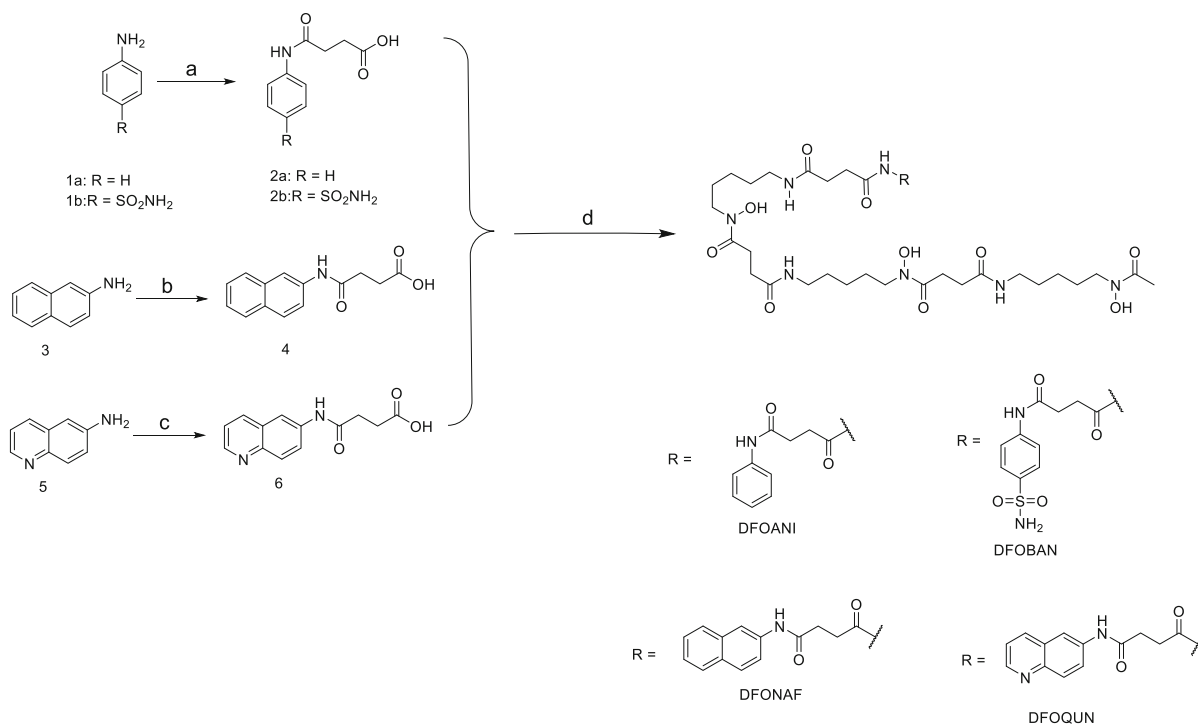
The coupling of DFO to carboxylic acids to prepare DFO-aniline (DFOANI), DFO-benzosulfanylamine (DFOBAN), DFO-2-naphthalenamine (DFO-NAF) and DFO-6-quinolinamine (DFOQUN) was performed (Scheme 1) according to described methods (Liu et al. 2010). Coupling was assisted by 1-ethyl-3-(3-dimethylaminopropyl)carbodiimide (EDC) and benzotriazol-1-ol (HOBt), which forms a tetrahedral intermediate that is a good leaving group. The crude products containing the desired compounds, as verified by RP-HPLC and mass spectrometry analyses, were purified by RP-HPLC to a limit of 250 mg per run. Difficulties in dissolving the products in the solvents used for this type of chromatography plus addition of DMSO to overcome such problems led to product losses and to relatively low purification yields. The conjugates were not sufficiently soluble in water or methanol to enable purification using flash chromatography and were thereafter purified using preparative RP-HPLC, with the following yields: DFOANI (27%), DFOBAN (25%), DFONAF (44%) and DFOQUN (24%). Techniques such as ¹H NMR, ¹³C NMR, UV-Vis and Mass Spectrometry were used to characterize both carboxylic acids precursors and the conjugates (see Supporting Information).

Calculation of lipophilicity of the conjugates was obtained by Marvin SketchTM. log P of DFONAF (0.05), DFOANI (-0.94) and DFOQUN (-0.78) were higher than water-soluble DFO (-2.02). This means that the addition of aromatic rings to DFO enhanced the hydrophobicity of the conjugates. Indeed, these conjugates were soluble only in DMSO. However, when a benzene ring has polar groups, such as in DFOBAN, hydrophilicity increased (log P = -2.34).

Iron binding and antioxidant studies

Calcein is a fluorescent probe with high affinity for Fe(III) (log K_{ML} = 24). Upon iron binding, the complex ferric calcein (CAFe) is formed, and its fluorescence is stoichiometrically (1:1) quenched. Being a stronger iron chelator than calcein, DFO (log K_{ML} = 30.6) scavenges iron and regenerates calcein fluorescence in a concentration-dependent manner (Espósito et al. 2002b).

The DFO conjugates under study, at physiological pH, displayed different binding patterns (Fig. 2a), suggesting that in some cases, the conjugation of aromatic rings to the DFO backbone altered the



Scheme 1 Schematic representation of the DFO conjugates syntheses. Reagents and conditions: **a** succinic anhydride, H₂O, 10 min, **b** succinic anhydride, H₂O, 15 min, **c** succinic

anhydride, reflux, Toluene, N₂(g), 4 h, **d** DFO, EDC, HOBT, DIPEA, DMF, N₂(g), RT, 16 h

coordination environment. The conjugate DFONAF did not display any fluorescence recovery, which may be a reflex of additional solubility problems (Ihnat et al. 2002). DFONAF was therefore excluded from further consideration as a MTDL chelator for brain iron. DFOANI is one ring smaller than DFONAF, and in this case we observed better fluorescence recovery, indicating that the metal has access to the otherwise unmodified tris(hydroxamate) binding site. DFOBAN presented also a high fluorescence recovery, possibly because the polar benzosulfanylamide group positively assists to the metal binding and at the same time does not hamper coordination (Ihnat et al. 2002). DFOQUN showed a binding pattern almost identical to that of DFO, indicating that the quinoline ring did neither attach to the tris(hydroxamate) binding site nor hamper metal approximation.

Iron-dependent oxidation processes occur in physiological conditions, and a very convenient and relevant form to assess antioxidants is the inspection of the effect of chelators in the dihydrorhodamine (DHR)/ascorbate system. This antioxidant test is based on the ability of redox-active iron species (such

as the ferric nitrilotriacetate, FeNTA) to participate in ROS-generating reactions mediated by ascorbate in a physiological buffer (HBS). The generated ROS will oxidize DHR, unless a suitable iron chelator is present in the medium (Espósito et al. 2003). Successful clinical chelators such as DFO can inhibit DHR oxidation (Fig. 2b), and any DFO-derived candidate drug should maintain the same ability. Except for DFONAF, this was verified for all conjugates, suggesting that they could potentially mitigate neurodegeneration promoted by iron-induced ROS generation (Chaston and Richardson 2003).

Finally, tests with the free radical 2,2-diphenyl-1-picrylhydrazyl (DPPH) (Molyneux 2004) showed that hydrogen atoms from all DFO conjugates are available for DPPH, as all of them behave as antioxidants (Fig. 3). Therefore, they can all confer antioxidant protection irrespective of their iron chelation efficacy.

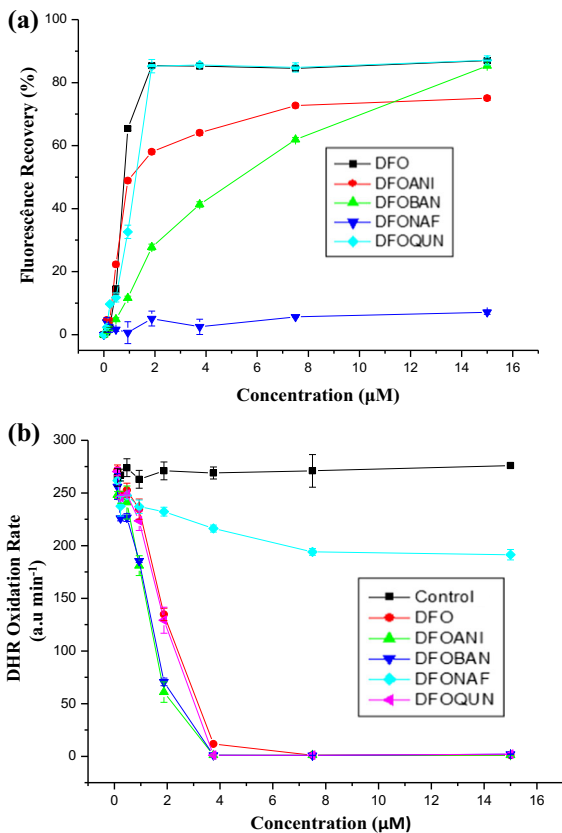


Fig. 2 **a** CAFe (2 µM) was treated with increasing concentrations of the conjugates (incubation time: 120 min). The experiment was repeated twice in duplicates. **b** Antioxidant activity of DFO conjugates against ascorbate oxidation catalyzed by iron. Fe(NTA) = 2 µM, Ascorbate = 40 µM, DHR = 50 µM. The experiment was repeated twice in duplicates

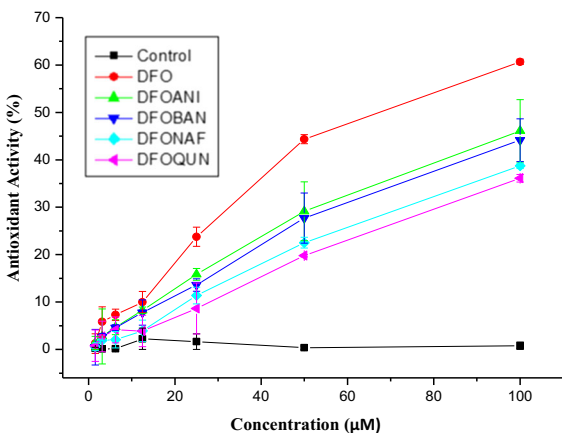


Fig. 3 Antioxidant activity of DFO conjugates (in DMSO) against 0.1 mM DPPH in methanol

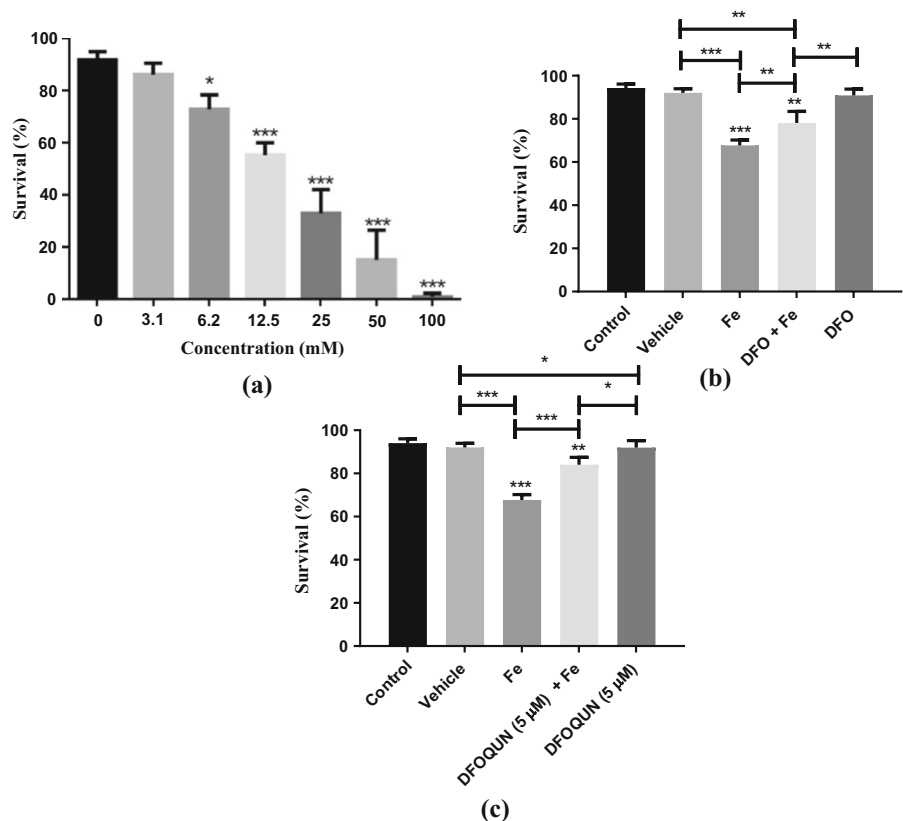
Lethality and survival assay in wild type *C. elegans*

Several iron compounds (such as iron chelates, zero-valent iron nanoparticles or iron salts) have been recognized to be neurotoxic in *C. elegans*. Ferrous sulfate at concentrations up to 2 mM has been found to negatively impact worm behavioral responses and neuronal viability (Fagundez et al. 2015; Hu et al. 2008; Soares et al. 2018). Therefore, the efficacy of the DFO conjugates in mitigating iron-induced damage was examined. First, we constructed a dose–response curve (Fig. 4a) to determine the optimal level for iron exposure. We selected a dose corresponding to half of the LC50, 6.2 mM, which lead to lethality in ~ 27% of the worms, and thus allowed us to test whether the effects of Fe might be reversible. Also, this concentration of free iron did not decrease the pH of the solution to toxic levels (higher FeSO₄ concentrations acidify the solution and increase toxicity). Under the aqueous, saline conditions employed, chemical speciation simulations (Supplementary Material) indicated that at 6.2 mM total iron, most of the metal would be in insoluble (hydro)oxide forms and only 0.9 µM would be soluble, and therefore bioavailable. This information guided us in the selection of DFO concentration (5 µM) that might revert iron-induced toxicity without being toxic themselves (Fig. 4b). Our results revealed that among the DFO conjugates, only DFOQUN performed the same as DFO in attenuating Fe-induced toxicity in the *C. elegans* model (Fig. 4c). DFOQUN by itself was not toxic. Interestingly, some authors described quinolines as promoters of the expression of superoxide dismutase, an important antioxidant enzyme (Salgueiro et al. 2014, 2017) and since DFOQUN is based on a quinoline, that could be an additional therapeutic effect. According to the positive results obtained, only DFOQUN was selected for subsequent testing in behavioral and mechanistic assays.

In vitro and in vivo AChE activity

Owing to the involvement of acetylcholinesterase (AChE) in the termination of signal transmission in the post-synaptic membranes, AChE inhibitors promote the accumulation of choline, and increase the duration of its effects, which are of interest for the treatment of AD symptoms (Lazarevic-Pasti et al. 2017). In this

Fig. 4 Iron toxicity and chelator activity in the N2 *C. elegans* strain. **a** Lethality induced by FeSO_4 ($\text{LC}_{50} = 13.6 \text{ mM}$). **b** Survival of worms treated with $5 \mu\text{M}$ DFO. **c** Survival of worms treated with $5 \mu\text{M}$ DFOQUN. For both **b** and **c**: $[\text{Fe}] = 6.2 \text{ mM}$; vehicle: 0.03% DMSO. All values are means \pm SD of $n = 3$ experiments performed in triplicate. Statistical analysis was carried out by means of one-way ANOVA, followed by Tukey's post hoc test. * $p < 0.05$, ** $p < 0.01$, *** $p < 0.001$; NS not significant



context, conjugation of an AChE inhibitor moiety (quinoline, inspired by tacrine) to an iron chelator could potentiate the effect of both compounds. Thus, in this study, AChE inhibition by the chelators was studied in vitro (AChE from *Electrophorus electricus*) and in *C. elegans* in vivo (Fig. 5). The results showed that DFOQUN significantly increased AChE inhibition compared to DFO (Fig. 5a; $p < 0.05$). Most likely, the quinoline moiety of DFOQUN blocks the docking of acetylcholine in the catalytic active site through π - π stacking interactions with residues such as phenylalanine and tryptophan (Chand et al. 2018; McKenna et al. 1997). Furthermore, in the presence of iron, the enzyme inhibition by DFO or DFOQUN was enhanced, suggesting that the complexes may have structural characteristics that may further contribute to their inhibitory effects. This is an intriguing possibility for the development of metal-based AChE inhibitors for the treatment of AD.

No difference in AChE inhibition was observed in *C. elegans* for both chelators at the concentrations studied (Fig. 5b). However, in the presence of iron the

chelators inhibited the enzyme more robustly (Fig. 5c). The similarity of effect between DFO and DFOQUN might be the result of metabolic deactivation, which should be confirmed in future metabolomics studies.

Finally, low concentrations of DMSO alone can increase peroxidase activity (by up to 10%), promoting resorufin production (Rammler 1967), which may account for the increased levels of AChE observed in the vehicle.

In vitro inhibition of $\text{A}\beta_{1-42}$ aggregation

The inhibitory capacity of DFO conjugates against $\text{A}\beta$ aggregation was studied with the thioflavin-T (ThT) assay. ThT is a dye that fluoresces upon binding to $\text{A}\beta$ fibrils; therefore, anti- $\text{A}\beta$ aggregation agents lead to reduced ThT fluorescence (Hayne et al. 2014). As expected, free iron increased $\text{A}\beta$ aggregation (Fig. 6). DFOQUN promoted greater inhibition of aggregation compared with DFO ($p < 0.01$), likely due to the presence of a lipophilic quinoline moiety in its

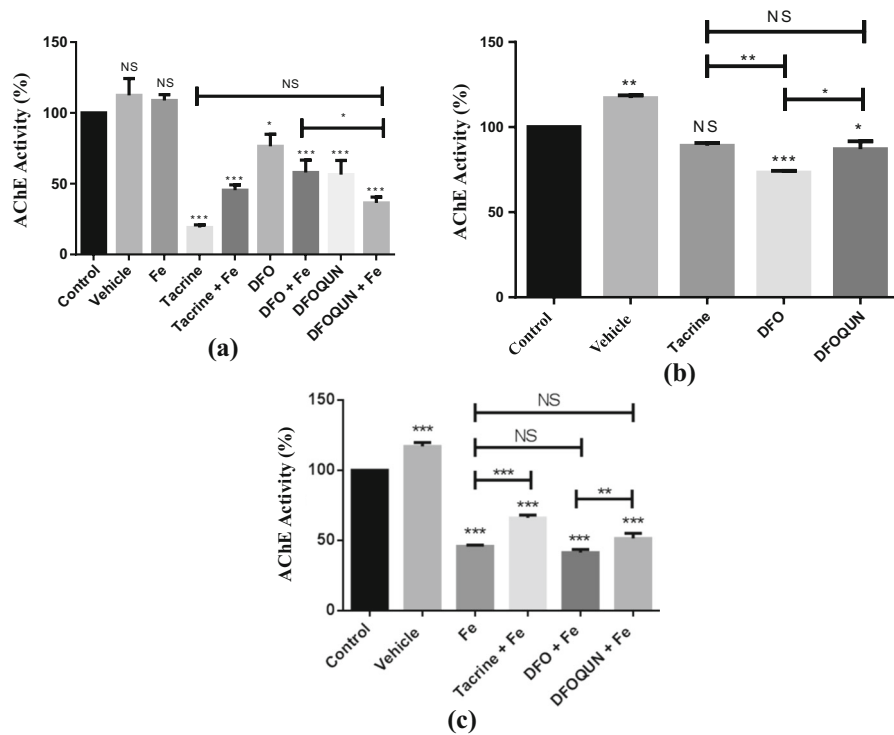


Fig. 5 Effect of the test compounds on AChE activity in the presence and absence of Fe(II). **a** in vitro test with AChE from *E. electricus* after 60 min incubation; [chelators] = [tacrine] = [Fe(II)] = 15 μM; vehicle = 0.1% DMSO. Tests with *C. elegans* were conducted in the absence **b** and presence **(c)** of 6.2 mM iron(II), and [chelators] = [

tacrine] = [Fe(II)] = 5 μM; vehicle = 0.03% DMSO; 15 min incubation. The values are means ± SD of n = 3 experiments performed in triplicate. Statistical analysis was carried out by means of one-way ANOVA, followed by Tukey’s post hoc test. *p < 0.05, **p < 0.01, ***p < 0.001. NS not significant

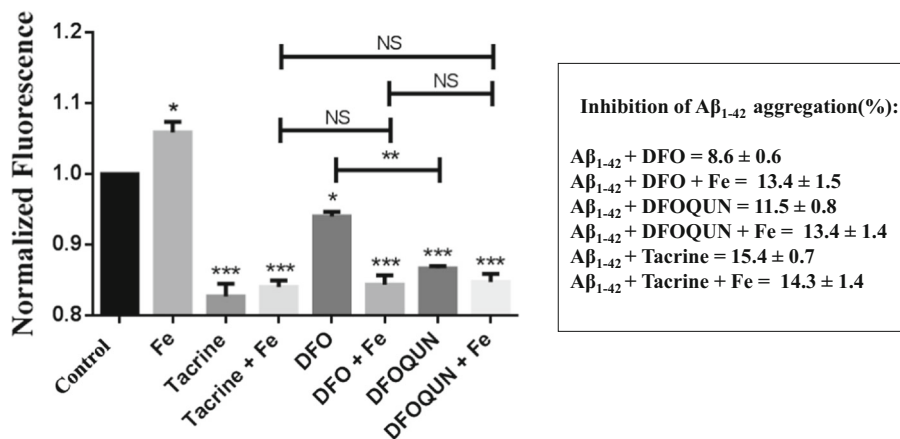


Fig. 6 Normalized fluorescence of thioflavin T probe. The values are means ± SD of n = 3 experiments performed in triplicate. Statistical analysis was carried out by means of one-way ANOVA, followed by Tukey’s post hoc test. *p < 0.05,

p < 0.01, *p < 0.001, NS = Not Significant. DFO, DFOQUN and tacrine = 20 μM; Aβ₁₋₄₂ = 1 μM; Fe(II) = 2 μM; DMSO percentage = 1%

structure. Indeed, tacrine, which was used as a positive control, also displayed inhibitory capacity (11.5%) of

peptide aggregation. This suggests that the conformation adopted by DFOQUN can disrupt β-sheet

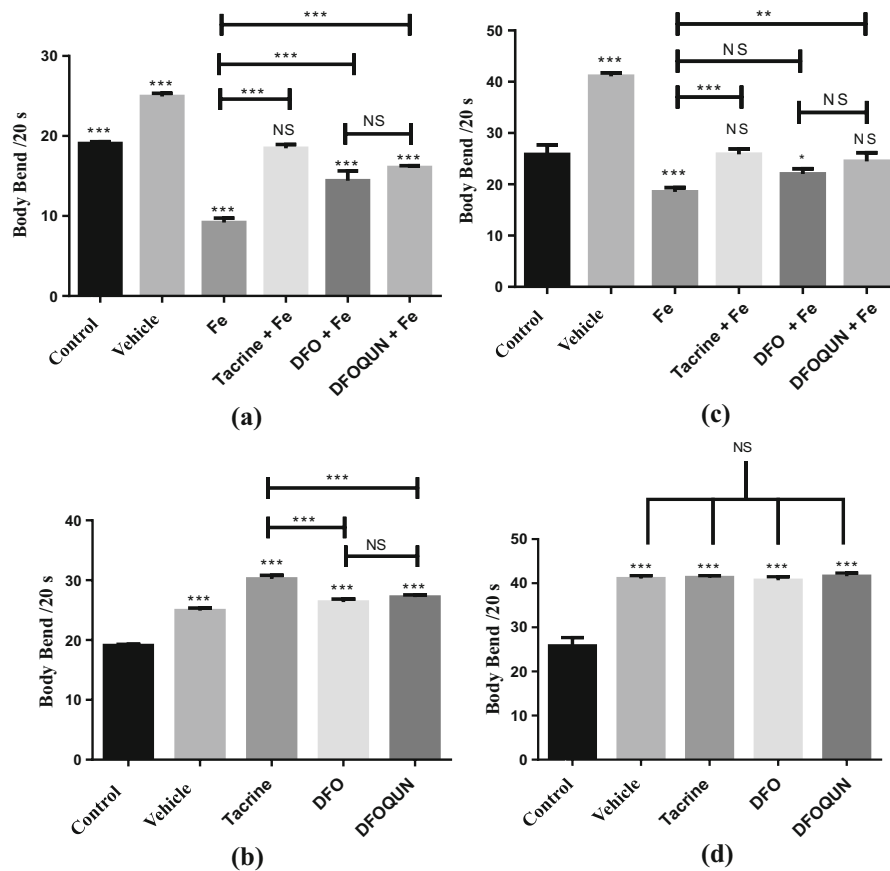


Fig. 7 Body bend assay in the N2 strain of *C. elegans* under starvation (**a, b**) or regular feeding (**c, d**), in the presence (**a, c**) or absence (**b, d**) of 6.2 mM iron. DFOQUN = DFO = Tacrine = 5 μ M. Vehicle = 0.03% DMSO. The values are means \pm SD

of $n = 3$ experiments performed in triplicate. Statistical analysis was carried out by means of one-way ANOVA, followed by Tukey's post hoc test. * $p < 0.05$, ** $p < 0.01$, *** $p < 0.001$, NS not significant

interactions of A β (Hiremathad et al. 2016; Quintanova et al. 2015a). Since the chelators are efficient iron scavengers, co-administration of iron with the chelators also did not lead to fibril aggregation.

DFO is a highly hydrophilic molecule, however, as is the case for other chelators, its metal complexes are more lipophilic due to the lower exposure of donor atoms to the solvent. Increased lipophilicity hampers the aggregation of A β , likely accounting for the fact that FeDFO has a greater anti-aggregation activity than DFO alone.

Body bend assay

Body bend assay in *C. elegans* was performed to assess locomotion deficits (Rand 2007). It is noteworthy that DMSO affects mechanoreceptor neurons,

altering their functions (Manalo and Medina 2020). As a defense mechanism, neurons will increase lys-7 expression (involved in defense responses in other organisms) and sod-5 expression (an ortholog of human superoxide dismutase 1; Manalo and Medina 2020; Wang et al. 2010). This process, in turn, will promote stress in the worms, increasing their locomotion frequency (see Fig. 7) as reflected by increased number of body bends for worms treated with vehicle when compared to saline controls.

Our results showed that under starvation (Fig. 7a, b) there was a significant recovery of motility loss caused by iron, when either chelators or tacrine ($p < 0.001$) were present at the same time (however, the locomotion levels were never the same as those for vehicle control, suggesting that simple DMSO disturbance was not the main effect). In the absence of iron-

induced stress, motility was higher and without significant differences between treatments. Under normal feeding (Fig. 7c, d) DFOQUN, but not DFO, promoted an increase in worm motility disturbed by iron (again, absent recovery to the levels of vehicle control). In this condition, again there was no significant differences between the worms exposed to tacrine, DFO and DFOQUN in the absence of iron-induced stress. Since acetylcholine plays an important role in neuromuscular junctions in *C. elegans* (Zamberlan et al. 2014), and iron-derived ROS can damage the cholinergic system, disrupting synapses between neurons and muscle cells (Gjorgjieva et al. 2014), it stands to reason that a dual iron chelator-AChE inhibitor such as DFOQUN would have a beneficial effect in ameliorating locomotor deficits in the iron-overloaded worms.

Conclusions

Of all the aromatic amine-desferrioxamine conjugates tested in this study, DFOQUN was of the highest interest given its ability to conserve both iron-binding and antioxidant capacities of the parent siderophore. In addition, co-administration of DFOQUN and iron also prevented Fe-induced toxicity in L1 *C. elegans*. When compared to the parent DFO, DFOQUN offered greater inhibition of both AChE activity and A β _{1–42} peptide aggregation. Finally, behavioral tests in *C. elegans* showed that DFOQUN was more efficient than DFO in reversing the Fe-induced motor impairment. These results provide impetus for the pursuit of dual function chelators and enzyme inhibitors as novel drugs for the treatment of metal-induced AD symptoms.

Acknowledgements This work was supported by FAPESP (2016/03709-9 and 2018/19684-0 to BPE and 2015/14360-4 to MTM) and CAPES (Brazilian agencies). MA was supported in part by grants from the National Institute of Environmental Health Science (NIEHS) R01ES07331 and R01ES10563.

Funding FAPESP 15/14360-4, 16/03709-9 and 18/19684-0; CAPES 88881.131918/2016-01; NIEHS R01ES07331 and R01ES10563.

Compliance with ethical standards

Conflict of interest The authors do not report conflicting interests.

References

- Alta ECP, Goswami D, Machini MT, Silvestre DM, Nomura CS, Espósito BP (2014) Desferrioxamine-caffeine (DFCAF) as a cell permeant moderator of the oxidative stress caused by iron overload. *Biometals* 27:1351–1360
- Arndt A, Liria CW, Yokoyama-Yasunaka JKU, Machini MT, Uliana SRB, Espósito BP (2017) New iminodibenzyl derivatives with anti-leishmanial activity. *J Inorg Biochem* 172:9–15. <https://doi.org/10.1016/j.jinorgbio.2017.04.004>
- Balakrishna D, Suryadevara V, Dandela R, Vegendla A, Mandava VBR, Manojit P (2014) Catalyst/surfactant free chemoselective acylation of amines in water current. *Green Chem* 1:73–79. <https://doi.org/10.2174/22133461114019990002>
- Berg L, Andersson CD, Artursson E, Hörnberg A, Tunemalm A-K, Linusson A, Ekström F (2011) Targeting acetylcholinesterase: identification of chemical leads by high throughput screening, struct determin mol modeling. *PLoS ONE* 6:e26039. <https://doi.org/10.1371/journal.pone.0026039>
- Bianchi L, Driscoll M (2006) Culture of embryonic *C. elegans* cells for electrophysiological and pharmacological analyses *WormBook*, ed. The *C. elegans* Research Community, *WormBook*, <https://doi.org/10.1895/wormbook.1.122.1>, <http://www.wormbook.org>.
- Brenner S (1974) The genetics of *Caenorhabditis elegans*. *Genetics* 77:71
- Breuer W, Hershko C, Cabantchik ZI (2000) The importance of non-transferrin bound iron in disorders of iron metabolism. *Transfus Sci* 23:185–192. [https://doi.org/10.1016/S0955-3886\(00\)00087-4](https://doi.org/10.1016/S0955-3886(00)00087-4)
- Cabantchik ZIS, Breuer W, Espósito BP (2013) The Molecular and cellular basis of iron toxicity in iron overload (io) disorders. *Diagn Ther Approaches Thalassemia Rep* 3:e3
- Chand K, Rajeshwari CE, Cardoso SM, Chaves S, Santos MA (2018) Tacrine–deferiprone hybrids as multi-target-directed metal chelators against Alzheimer’s disease: a two-in-one drug. *Metallomics* 10:1460–1475. <https://doi.org/10.1039/C8MT00143J>
- Chaston TB, Richardson DR (2003) Iron chelators for the treatment of iron overload disease: relationship between structure, redox activity, and toxicity. *Am J Hematol* 73:200–210. <https://doi.org/10.1002/ajh.10348>
- Chen T, Li M, Liu J (2018a) π – π stacking interaction: a non-destructive and facile means in material engineering for bioapplications. *Cryst Growth Des* 18:2765–2783. <https://doi.org/10.1021/acs.cgd.7b01503>
- Chen Y et al (2018b) Synthesis and bioevaluation of new tacrine-cinnamic acid hybrids as cholinesterase inhibitors against Alzheimer’s disease. *J Enzyme Inhib Med Chem* 33:290–302. <https://doi.org/10.1080/14756366.2017.1412314>
- Colović MB, Krstić DZ, Lazarević-Pašti TD, Bondžić AM, Vasić VM (2013) Acetylcholinesterase inhibitors: pharmacology and toxicology. *Curr Neuropharmacol* 11:315–335. <https://doi.org/10.2174/1570159X11311030006>

- Espósito BP, Breuer W, Cabantchik ZI (2002a) Design and applications of methods for fluorescence detection of iron in biological systems. *Biochem Soc Trans* 30:729–732
- Espósito BP, Epsztejn S, Breuer W, Cabantchik ZI (2002b) A review of fluorescence methods for assessing labile iron in cells and biological fluids. *Anal Biochem* 304:1–18. <https://doi.org/10.1006/abio.2002.5611>
- Espósito BP, Breuer W, Sirankapracha P, Pootrakul P, Hershko C, Cabantchik ZI (2003) Labile plasma iron in iron overload: redox activity and susceptibility to chelation. *Blood* 102:2670–2677. <https://doi.org/10.1182/blood-2003-03-0807>
- Espósito BP, Martins AC, Carvalho RRV, Aschner M (2020) High throughput fluorimetric assessment of iron traffic and chelation in iron-overloaded *Caenorhabditis elegans*. *Biometals* 33:255–327. <https://doi.org/10.1007/s10534-020-00250-4>
- Fagundez DDA et al (2015) Behavioral and dopaminergic damage induced by acute iron toxicity in *Caenorhabditis elegans*. *Toxicol Res* 4:878–884. <https://doi.org/10.1039/C4TX00120F>
- Gjorgjieva J, Biron D, Haspel G (2014) Neurobiology of *Caenorhabditis elegans* locomotion: where do we stand? *Bioscience* 64:476–486. <https://doi.org/10.1093/biosci/biu058>
- Goswami D, Machini MT, Silvestre DM, Nomura CS, Espósito BP (2014) Cell Penetrating Peptide (CPP)-conjugated desferrioxamine for enhanced neuroprotection: synthesis and in vitro evaluation bioconjugate. *Chemistry* 25:2067–2080. <https://doi.org/10.1021/bc5004197>
- Guzior N, Bajda M, Rakoczy J, Brus B, Gobec S, Malawska B (2015) Isoindoline-1,3-dione derivatives targeting cholinesterases: design, synthesis and biological evaluation of potential anti-Alzheimer's agents. *Bioorg Med Chem* 23:1629–1637. <https://doi.org/10.1016/j.bmc.2015.01.045>
- Hart AC (2006) Behavior
- Hayne DJ, Lim S, Donnelly PS (2014) Metal complexes designed to bind to amyloid- β for the diagnosis and treatment of Alzheimer's disease. *Chem Soc Rev* 43:6701–6715. <https://doi.org/10.1039/C4CS00026A>
- Heli H, Mirtorabi S, Karimian K (2011) Advances in iron chelation: an update. *Expert Opin Ther Pat* 21:819–856. <https://doi.org/10.1517/13543776.2011.569493>
- Hider RC, Roy S, Ma YM, Le Kong X, Preston J (2011) The potential application of iron chelators for the treatment of neurodegenerative diseases. *Metallomics* 3:239–249. <https://doi.org/10.1039/C0MT00087F>
- Hiremathad A et al (2016) Tacrine-allyl/propargylcysteine-benzothiazole trihybrids as potential anti-Alzheimer's drug candidates. *RSC Adv* 6:53519–53532. <https://doi.org/10.1039/C6RA03455A>
- Hu Y-O, Wang Y, Ye B-P, Wang D-Y (2008) Phenotypic and behavioral defects induced by iron exposure can be transferred to progeny in *Caenorhabditis elegans*. *Biomed Environ Sci* 21:467–473. [https://doi.org/10.1016/S0895-3988\(09\)60004-0](https://doi.org/10.1016/S0895-3988(09)60004-0)
- Ihnat PM, Vennerstrom JL, Robinson DH (2002) Solution equilibria of deferoxamine amides. *J Pharm Sci* 91:1733–1741. <https://doi.org/10.1002/jps.10168>
- Kenyon C (1988) The nematode *Caenorhabditis elegans*. *Science* 240:1448–1453. <https://doi.org/10.1126/science.3287621>
- Keri RS, Quintanova C, Marques SM, Esteves AR, Cardoso SM, Santos MA (2013) Design, synthesis and neuroprotective evaluation of novel tacrine-benzothiazole hybrids as multi-targeted compounds against Alzheimer's disease. *Bioorg Med Chem* 21:4559–4569. <https://doi.org/10.1016/j.bmc.2013.05.028>
- Keri RS, Quintanova C, Chaves S, Silva DF, Cardoso SM, Santos MA (2016) New tacrine hybrids with natural-based cysteine derivatives as multitargeted drugs for potential treatment of Alzheimer's disease. *Chem Biol Drug Des* 87:101–111. <https://doi.org/10.1111/cbdd.12633>
- Knutson MD (2019) Non-transferrin-bound iron transporters. *Free Radic Biol Med* 133:101–111. <https://doi.org/10.1016/j.freeradbiomed.2018.10.413>
- Kozłowski H, Luczkowski M, Remelli M, Valensin D (2012) Copper, zinc and iron in neurodegenerative diseases (Alzheimer's, Parkinson's and prion diseases) coordination. *Chem Rev* 256:2129–2141. <https://doi.org/10.1016/j.ccr.2012.03.013>
- Kurth C, Kage H, Nett M (2016) Siderophores as molecular tools in medical and environmental applications. *Org Biomol Chem* 14:8212–8227. <https://doi.org/10.1039/C6OB01400C>
- Lazarevic-Pasti T, Leskovic A, Momic T, Petrovic S, Vasic V (2017) Modulators of acetylcholinesterase activity: from Alzheimer's disease to anti-cancer drugs. *Curr Med Chem* 24:3283–3309. <https://doi.org/10.2174/0929867324666170705123509>
- Liu J et al (2010) Conjugates of desferrioxamine B (DFOB) with derivatives of adamantane or with orally available chelators as potential agents for treating iron overload. *J Med Chem* 53:1370–1382. <https://doi.org/10.1021/jm9016703>
- Manalo RVM, Medina PMB (2020) Caffeine reduces deficits in mechanosensation and locomotion induced by L-DOPA and protects dopaminergic neurons in a transgenic *Caenorhabditis elegans* model of Parkinson's disease. *J Pharm Bil* 58:721–731. <https://doi.org/10.1080/13880209.2020.1791192>
- Maqbool M, Rajvansh R, Srividya K, Hoda N (2020) Deciphering the robustness of pyrazolo-pyridine carboxylate core structure-based compounds for inhibiting α -synuclein in transgenic *C. elegans* model of Synucleinopathy. *Bioorg Med Chem* 28:115640
- Martinez CR, Iverson BL (2012) Rethinking the term “pi-stacking.” *Chem Sci* 3:2191–2201. <https://doi.org/10.1039/C2SC20045G>
- McKenna MT, Proctor GR, Young LC, Harvey AL (1997) Novel tacrine analogues for potential use against Alzheimer's disease: potent and selective acetylcholinesterase inhibitors and 5-HT uptake inhibitors. *J Med Chem* 40:3516–3523. <https://doi.org/10.1021/jm970150t>
- Molyneux P (2004) The use of the stable radical Diphenylpicrylhydrazyl (DPPH) for estimating antioxidant activity Songklanakarin. *J Sci Technol* 26:212–219
- Palleria C, Di Paolo A, Giofrè C, Caglioti C, Leuzzi G, Siniscalchi A, De Sarro G, Gallelli L (2013) Pharmacokinetic drug-drug interaction and their implication in clinical management. *J Res Med Sci* 18:601–610

- Piemontese L et al (2018) Donepezil structure-based hybrids as potential multifunctional anti-Alzheimer's drug candidates. *J Enzyme Inhib Med Chem* 33:1212–1224. <https://doi.org/10.1080/14756366.2018.1491564>
- Pramanik S, Chakraborty S, Sivan M, Patro BS, Chatterjee S, Goswami D (2019) Cell permeable imidazole-desferrioxamine conjugates: synthesis and in vitro evaluation. *Bioconj Chem* 30:841–852. <https://doi.org/10.1021/acs.bioconjchem.8b00924>
- Quintanova C, Keri R, Chaves S, Santos MA (2015a) Copper(II) complexation of tacrine hybrids with potential anti-neurodegenerative roles. *J Inorg Biochem*. <https://doi.org/10.1016/j.jinorgbio.2015.06.008>
- Quintanova C, Keri RS, Marques SM, Maria G, Cardoso SM, Serralheiro ML, Santos MA (2015b) Design, synthesis and bioevaluation of tacrine hybrids with cinnamate and cinnamylidene acetate derivatives as potential anti-Alzheimer drugs. *MedChemComm* 6:1969–1977. <https://doi.org/10.1039/C5MD00236B>
- Raines DJ, Sanderson TJ, Wilde EJ, Duhme-Klair AK (2015) Siderophores. In: Reference module in chemistry, molecular sciences and chemical engineering. Elsevier. <https://doi.org/10.1016/B978-0-12-409547-2.11040-6>
- Rammler DH (1967) The effect of DMSO on several enzyme systems. *Ann N Y Acad Sci* 141:291–299. <https://doi.org/10.1111/j.1749-6632.1967.tb34893.x>
- Rand JB (2007) Acetylcholine WormBook (ed) The C. elegans Research Community, WormBook, <https://doi.org/10.1895/wormbook.1.131.1>, <http://www.wormbook.org>.
- Riwar L-J, Trapp N, Kuhn B, Diederich F (2017) Substituent effects in parallel-displaced π - π stacking interactions: distance matters. *Angew Chem Int Ed* 56:11252–11257. <https://doi.org/10.1002/anie.201703744>
- Rodríguez-Rodríguez C, Telpoukhovskaia M, Orvig C (2012) The art of building multifunctional metal-binding agents from basic molecular scaffolds for the potential application in neurodegenerative diseases. *Coord Chem Rev* 256:2308–2332. <https://doi.org/10.1016/j.ccr.2012.03.008>
- Salgueiro WG et al (2014) Direct synthesis of 4-organyl-sulfenyl-7-chloro quinolines and their toxicological and pharmacological activities in *Caenorhabditis elegans*. *Eur J Med Chem* 75:448–459. <https://doi.org/10.1016/j.ejmech.2014.01.037>
- Salgueiro WG et al (2017) Insights into the differential toxicological and antioxidant effects of 4-phenylchalcogenil-7-chloroquinolines in *Caenorhabditis elegans*. *Free Radic Biol Med* 110:133–141. <https://doi.org/10.1016/j.freeradbiomed.2017.05.020>
- Santos MA, Chand K, Chaves S (2016) Recent progress in multifunctional metal chelators as potential drugs for Alzheimer's disease. *Coord Chem Rev* 327–328:287–303. <https://doi.org/10.1016/j.ccr.2016.04.013>
- Sashidhara KV, Modukuri RK, Jadiya P, Rao KB, Shjarma T, Haque R, Singh DK, Banerjee D, Siddiqi MI, Nazir A (2014a) Discovery of 3-arylcoumarin-tetracyclic tacrine hybrids as multifunctional agents against Parkinson's disease. *ACS Med Chem Lett* 5:1099–1103
- Sashidhara KV et al (2014b) Benzofuran-chalcone hybrids as potential multifunctional agents against Alzheimer's disease: synthesis and in vivo studies with transgenic *Caenorhabditis elegans*. *ChemMedChem* 9:2671–2684. <https://doi.org/10.1002/cmdc.201402291>
- Schneider L (2000) A critical review of cholinesterase inhibitors as a treatment modality in Alzheimer's disease. *Dialogues Clin Neurosci* 2:111–128
- Sheth S (2014) Iron chelation: an update. *Curr Opin Hematol* 21:179–185. <https://doi.org/10.1097/moh.000000000000031>
- Sinha SK, Shrivastava SK (2013) Design, synthesis and evaluation of some new 4-aminopyridine derivatives in learning and memory. *Bioorg Med Chem Lett* 23:2984–2989. <https://doi.org/10.1016/j.bmcl.2013.03.026>
- Soares MV, Puntel RL, Ávila DS (2018) Resveratrol attenuates iron-induced toxicity in a chronic post-treatment paradigm in *Caenorhabditis elegans*. *Free Radic Res* 52:939–951. <https://doi.org/10.1080/10715762.2018.1492119>
- Thakuria R, Nath NK, Saha BK (2019) The nature and applications of π - π interactions: a perspective. *Cryst Growth Des* 19:523–528. <https://doi.org/10.1021/acs.cgd.8b01630>
- Tiiman A, Palumaa P, Tõugu V (2013) The missing link in the amyloid cascade of Alzheimer's disease—metal ions. *Neurochem Int* 62:367–378. <https://doi.org/10.1016/j.neuint.2013.01.023>
- Walaszek M, Del Nero M, Bois P, Ribstein L, Courson O, Wanko A, Laurent J (2018) Sorption behavior of copper, lead and zinc by a constructed wetland treating urban stormwater. *Appl Geochem* 97:167–180. <https://doi.org/10.1016/j.apgeochem.2018.08.019>
- Wang X, Wang X, Li L, Wang D (2010) Lifespan extension in *Caenorhabditis elegans* by DMSO is dependent on sir-2.1 and daf-16. *Biochem Biophys Res Commun* 400:613–618. <https://doi.org/10.1016/j.bbrc.2010.08.113>
- Ward RJ, Dexter DT, Crichton RR (2015) Neurodegenerative diseases and therapeutic strategies using iron chelators. *J Trace Elem Med Biol* 31:267–273. <https://doi.org/10.1016/j.jtemb.2014.12.012>
- Xie RJ, Tan EK, Puah AN (2009) Oxidation-reduction potential in saline water reverse osmosis membrane desalination and its potential use for system control. *Desalin Water Treat* 3:193–203. <https://doi.org/10.5004/dwt.2009.460>
- Zamberlan DC, Arantes LP, Machado ML, Golombieski R, Soares FAA (2014) Diphenyl-diselenide suppresses amyloid- β peptide in *Caenorhabditis elegans* model of Alzheimer's disease. *Neuroscience* 278:40–50. <https://doi.org/10.1016/j.neuroscience.2014.07.068>

Publisher's Note Springer Nature remains neutral with regard to jurisdictional claims in published maps and institutional affiliations.